Article

Identifying the Spatial Range of the Pearl River Delta Urban Agglomeration from a Differentiated Perspective of Population Distribution and Population Mobility

Yongwang Cao [1,2,†] , Qingpu Li [3,†] and Zaigao Yang [1,*]

1   Guangzhou Academy of Social Sciences, Guangzhou 510410, China; caoyw6@mail2.sysu.edu.cn
2   School of Economics and Finance, South China University of Technology, Guangzhou 510006, China
3   Institute of International Rivers and Eco-Security, Yunnan University, Kunming 650500, China; 22024127015@stu.ynu.edu.cn
*   Correspondence: yzgao@gz.gov.cn; Tel.:+86-020-86464381
†   These authors contributed equally to this work.

Abstract: Accurate identification of urban agglomeration spatial range is essential for scientific regional planning, optimal resource allocation, and sustainable development, forming the basis for regional development policy. To improve the accuracy of identifying urban agglomeration boundaries, this study fuses nighttime light data, which reflects urban economic levels, with LandScan data representing population distribution and heatmap data indicating population mobility. This fusion allows for identification from a differentiated perspective of population distribution and mobility. We propose a new method for identifying the dynamic boundaries of urban agglomerations through multi-source data fusion. This method not only provides technical support for scientific regional planning but also effectively guides the functional positioning of edge cities and the optimization of resource allocation. The results show that the spatial range identified by NTL_LS has an accuracy of 80.37% and a kappa coefficient of 0.5225, while NTL_HM achieves an accuracy of 89.17% with a kappa coefficient of 0.7342, indicating that the fusion of economic level with population mobility data more accurately reflects the spatial range of urban agglomerations in line with real development patterns. By adopting a differentiated perspective on population distribution and mobility, we propose a new approach to identifying urban agglomeration spatial range. The research results based on this method provide more comprehensive and dynamic decision-making support for optimizing transportation layouts, allocating public resources rationally, and defining the functional positioning of edge cities.

Keywords: Pearl River Delta urban agglomeration; urban spatial range; differentiation; population distribution; population mobility

1. Introduction

Urban agglomerations refer to a collection of cities centered around one or more major cities, with surrounding cities closely connected through economic, social, and transportation links [1]. As highly concentrated urban entities, urban agglomerations play a significant role in national and regional development, serving as a key driver for regional coordinated growth and efficient economic expansion [2]. However, during the development of urban agglomerations, issues such as unclear boundaries, ambiguous functional zoning within the agglomeration, and excessive concentration of resources in core cities

have gradually emerged. These challenges not only hinder the sustainable development of urban agglomerations but also present obstacles to regional coordination [3,4]. Therefore, in order to address these problems more effectively, it is essential to accurately identify the spatial range of urban agglomerations, enabling the exploration of how precise identification of spatial boundaries can facilitate optimized resource allocation and regional collaborative development. Since the 1980s, China has undergone a large-scale urbanization process characterized by massive rural-to-urban migration and the high concentration of economic resources in urban areas. This rapid urbanization has elevated the status of China's urban agglomerations, such as the Pearl River Delta, Beijing–Tianjin–Hebei, and the Yangtze River Delta, within the global urban network [5,6]. The Pearl River Delta, in particular, has attracted significant inflows of population and capital due to its favorable geographic location and its role as a global manufacturing hub. This has resulted in a high-intensity economic interaction zone centered around the Guangzhou–Shenzhen corridor. This urbanization process has not only shaped the regional economic structure within China but also had profound implications for the East Asian and global economic systems. Pentland et al. highlight that one key feature of China's rapid urbanization is the dual driving forces of globalization and regionalization. Through the clustering of regional urban agglomerations, China has optimized resource allocation among regions domestically while also becoming an integral part of the global value chain. This dynamic characteristic serves as a crucial context for urban agglomeration studies [7].

The spatial range of an urban agglomeration refers to a functionally integrated area comprising a core city and its surrounding regions, closely linked in terms of geography, economy, and society [8]. This range is typically determined by factors such as population distribution, economic activity density, and transportation networks, and it continuously adapts in response to urban expansion and changes in functional zones [9,10]. The definitions of terms related to urban agglomerations may vary under different research contexts. For example, a metropolitan area usually refers to the extended area of a single city, where economic activities and population mobility are primarily concentrated in the core city and its suburban areas. A functional area, on the other hand, emphasizes the functional network characteristics that span administrative boundaries, such as transportation connections and economic integration. The concept of conurbation highlights the overlapping boundaries of multiple cities in geographic space, while urban agglomeration focuses on the networked structure formed through economic, social, and transportation linkages between cities. Moreover, the term economic functional area describes cross-regional development corridors driven primarily by economic activities characterized by high levels of industrial agglomeration. In contrast, a metropolitan region combines geographic and economic characteristics, typically including one or more urban centers and their surrounding functional areas [11–14]. The definition of urban agglomeration boundaries involves multiple disciplinary fields, including spatial modeling, urban morphology, and regional economics. Spatial autocorrelation theory analyzes the similarity of geographic features, revealing spatial connections and boundary characteristics between cities [15]. For example, the Spatial Durbin Model (SDM) is widely used to examine the diffusion and spillover effects of economic activities within urban agglomerations [5]. At the same time, network theory conceptualizes urban agglomerations as complex networks composed of multiple nodes (cities) and edges (economic or transportation links), highlighting functional interactions and spatial structures between cities [16]. These theories provide important conceptual support for identifying the spatial boundaries of urban agglomerations. Traditionally, the spatial boundaries of urban agglomerations have been delineated based on administrative boundaries. However, this static approach often fails to accommodate the complex, dynamic interactions within urban agglomerations, primarily because adminis-

trative boundaries do not necessarily reflect the actual functional division and interactions within the agglomeration [17,18]. Additionally, administrative boundaries overlook cross-regional economic activities and population mobility, leading to misinterpretations of the agglomeration's true spatial range and structure [19]. Thus, a more accurate identification of the spatial boundaries of urban agglomerations requires a comprehensive analysis based on multi-dimensional data, including economic activity, population distribution, and mobility.

The spatial range of urban agglomerations is closely linked to economic development and population mobility. The concentration and expansion of economic activities drive the spatial range of urban agglomerations, impacting not only the physical expansion but also the layout of functional zones [20,21]. Economic activities such as industrial distribution and infrastructure investment directly influence the direction and scale of urban agglomeration delineation. Analyzing economic factors can reveal the levels of economic activity in different areas of the agglomeration, thereby identifying the spatial and temporal trends in its boundary shifts [22,23]. On the other hand, population plays an equally crucial role in defining the spatial range of urban agglomerations [24]. Firstly, changes in the resident population reflect long-term settlement and concentration of economic activities within the agglomeration, influencing functional zoning and determining the core structure of the agglomeration [25]. Secondly, the mobility of the population through migration reveals economic connections between regions, prompting dynamic adjustments in the spatial boundaries of urban agglomerations [26]. Therefore, in the development of urban agglomerations, the interaction between economic growth and population dynamics determines both the scale and direction of the spatial range. In recent years, the Global Human Settlement Layer (GHSL), as a global approach based on satellite imagery and spatial modeling, has been widely applied in urban spatial identification. GHSL provides a unified global perspective that allows for the analysis of spatial changes in urban morphology across regional differences. It also effectively reflects the boundaries and structural characteristics of cities in different areas. Compared to traditional methods based on economic or population data, GHSL integrates multi-source remote sensing data and a global analytical framework, offering significant advantages in capturing the dynamic evolution of urban agglomerations, cross-regional connections, and morphological distribution patterns [27]. Studies using GHSL data have analyzed the boundary dynamics of major urban agglomerations in Europe, revealing the interaction between urban morphology and transportation networks [28]. Furthermore, the application of GHSL in functional area division provides a useful reference framework for the rapidly developing East Asian region [28].

Previous approaches for identifying the spatial range of urban agglomerations from an economic perspective include spatial econometric models, multi-level regression analysis, and urban growth boundary models [29,30]. These approaches reveal the spatial characteristics of urban agglomerations by analyzing inter-city economic interactions, spillover effects, and the impact of economic activities on land use and spatial structure [31]. Some scholars have applied spatial autocorrelation models and Spatial Durbin Models (SDMs) to analyze economic linkages and spillover effects among cities [32], while others have employed Hierarchical Linear Models (HLMs) to explore economic growth factors at different scales [33]. The data used in these studies mainly include macroeconomic indicators, spatial economic data, transportation and logistics data, and regional policy data, which help delineate the spatial range of urban agglomerations through insights into economic activity, industrial division, transportation infrastructure, and policy influence [34,35]. Some studies use land use and housing price data to analyze urban agglomeration boundaries [36], while others assess the impact of infrastructure using transportation data [17]. However, these traditional data sources lack sufficient temporal and spatial precision, as well as

real-time accuracy, making it difficult to accurately capture the dynamic changes in urban agglomerations. Nighttime light (NTL) data, which reflects economic activity and spatial development patterns, has been widely applied to identifying urban spatial boundaries [37]. Nevertheless, limitations such as spillover effects and limited spatial resolution of NTL data still restrict their precision in defining urban boundaries [38].

From a demographic perspective, methods for identifying the spatial range of urban agglomerations include analyses of population density and spatial distribution, migration patterns, age structure, occupational distribution, and housing demand [39]. Researchers utilize data on population density, migrant populations, age structure, and housing demand to reveal the population dynamics and characteristics that inform the spatial delineation of urban agglomerations [40]. Some studies analyze housing demand data to define the spatial boundaries of urban agglomerations, while others explore the effects of population concentration [41]. Among the widely used population distribution datasets is LandScan, a global population dataset that enables the rapid identification of densely populated areas within urban agglomerations, thus helping to define their spatial boundaries [42–44]. However, LandScan data also face limitations, such as insufficient resolution and low update frequency, which constrain its applicability in dynamic change analysis. In recent years, scholars have begun to fuse economic and demographic perspectives to identify urban spatial boundaries more comprehensively [45,46]. This approach provides a more holistic view of urban agglomeration analysis [47]. Currently, many studies employ data fusion methods, combining NTL data with LandScan data [48]. NTL data reflect the intensity of economic activity, while LandScan data display resident population distribution, making it relatively more accurate to delineate urban agglomeration boundaries by combining both sources [49]. However, it is important to note that the increasing mobility of population factors within urban agglomerations complicates reliance on resident population data alone for boundary identification, especially as migrant populations have an increasingly significant impact on urban economic and social dynamics [50]. Overall, urban agglomeration boundary identification methods based on remote sensing imagery have been widely applied, with NTL data being a common source due to their ability to visually reflect the distribution of economic activity [51]. However, NTL data suffer from spillover effects, making it difficult to precisely identify economic activities in peripheral areas [52]. In comparison, LandScan data provide a static perspective on urban agglomeration through high-resolution population distribution information, but their lack of dynamic features limits their ability to capture short-term changes [53]. In recent years, heatmap data have become an important source for identifying the dynamic boundaries of urban agglomerations due to their ability to capture real-time population mobility. This study fuses NTL, LandScan, and heatmap data, combining the dynamic characteristics of economic activity, population distribution, and mobility. It proposes an innovative method to identify urban agglomeration boundaries from a multi-dimensional perspective.

With the advancement of big data, the collection of population mobility data has become increasingly feasible. Data sources such as mobile device location data, social media sign-ins, and transit card swipe records are now used to analyze population flows and spatial structures [54–56]. To further enhance the accuracy of urban spatial boundary identification, researchers are increasingly incorporating various big data sources, such as Points of Interest (POI) data and transportation data, which provide detailed information on the distribution of functional zones and patterns of human activity within cities [57]. However, static data often fail to fully capture real-time population mobility patterns, leading to increased attention to heatmap data that can reflect real-time population flows [58]. Heatmap data, based on geolocation information, visually depict the intensity and distribution of human activity within specific areas. Observing macro-level mobility trends helps identify

functional areas and boundaries between cities, effectively capturing dynamic interactions within a region [59]. Heatmap data allow for an intuitive analysis of high-frequency population mobility paths and hotspot areas, revealing the actual intensity of connections across city boundaries. For example, in the Pearl River Delta region, the intensity of population mobility along the Guangzhou–Shenzhen corridor reflects not only economic activities but also serves as an important basis for defining functional areas. Compared to static administrative boundaries, boundary identification methods based on dynamic mobility data offer greater flexibility. By integrating heatmap data, researchers can better represent dynamic population flows within urban agglomerations, offering a more accurate and flexible approach to identifying urban agglomeration boundaries, especially in areas with dense migrant populations. This method significantly improves the precision and reliability of urban agglomeration boundary identification [60,61], thereby providing a more scientific basis for urban development and policymaking. Although existing studies propose various methods to identify the spatial boundaries of urban agglomerations, including spatial econometric models based on economic activities, urban expansion models based on land use changes, and dynamic analysis methods based on population distribution, these approaches have notable limitations. Methods relying on a single data source often fail to capture cross-boundary connections and dynamic changes between regions [45]. Moreover, many studies heavily depend on administrative boundaries or resident population distribution data, whose static characteristics make them unsuitable for addressing the complex dynamics of rapid urbanization and population mobility [62]. To address these issues, this study fuses multi-source data (NTL data, LandScan data, and heatmap data) and adopts a dual perspective of economic activity and population mobility. This approach provides a more comprehensive method for identifying the spatial boundaries of urban agglomerations, overcoming the shortcomings of existing methods in terms of dynamism and applicability.

This study selects the Pearl River Delta (PRD) urban agglomeration as a case study, integrating NTL, LandScan population distribution data, and heatmap data to identify the spatial range of the urban agglomeration. First, by fusing NTL and LandScan data, an NTL_LandScan dataset is created to delineate the spatial boundaries of the PRD urban agglomeration. Next, an NTL_Heatmap dataset is generated by combining NTL and heatmap data to further refine the identification of the urban agglomeration's spatial range. Finally, the identification results from the NTL_LandScan and NTL_Heatmap datasets are subjected to accuracy validation and comparative analysis. By fusing NTL, LandScan, and heatmap data, we aim to systematically explore the identification of urban agglomeration spatial boundaries from a perspective that combines static and dynamic analyses. This approach addresses the limitations of traditional methods based on a single data source, offering significant advantages, particularly in capturing cross-regional dynamic connections and high mobility characteristics. It also enables a more accurate identification of the spatial boundaries of the Pearl River Delta urban agglomeration from different perspectives. Furthermore, it provides reliable references for resource allocation and regional development in the Pearl River Delta, contributing to its sustainable development.

2. Materials and Methods

2.1. Study Area

The PRD urban agglomeration is located in the southern part of Guangdong Province, China, and is one of the most economically active and densely populated urban agglomerations in the country (Figure 1). The PRD includes nine major cities—Guangzhou, Shenzhen, Foshan, Dongguan, Zhuhai, Zhongshan, Huizhou, Jiangmen, and Zhaoqing—covering a

total area of approximately 56,000 square kilometers. The PRD is highly representative of urban agglomeration development in China. In 2023, the combined GDP of these nine cities reached 11.02 trillion RMB, accounting for 81.24% of Guangdong's GDP and approximately 8.81% of the national GDP. This high economic concentration positions the PRD as a crucial link for the aggregation and diffusion of production factors between regions, establishing a unique model of economic interaction. As of 2023, the PRD's permanent population exceeded 86 million, making it one of the most densely populated and dynamic regions in terms of population mobility in China [63]. The continued expansion of the PRD has not only fueled regional economic growth but also introduced complex challenges in urban functional zoning and resource allocation. Therefore, this study employs both economic and demographic perspectives to identify and analyze the dynamic changes in the spatial range of the PRD urban agglomeration, aiming to reveal its functional structure and spatial boundary characteristics amid rapid development.
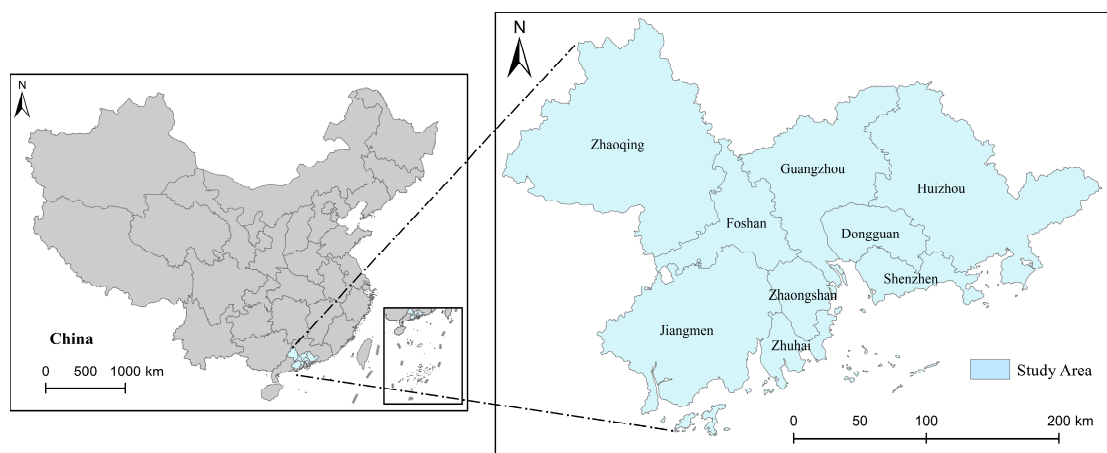

Figure 1. Study Area.

2.2. Study Data

The data used in this study primarily include NTL data, LandScan data, and heatmap data. The specific processing methods and workflow for each type of data are detailed as follows (Table 1):

Table 1. Data attribute.

Data Type	Data Source	Advantages	Limitations	Processing Steps
Nighttime Light Data (NTL)	NPP-VIIRS (NASA/NOAA)	Reflects economic activity intensity; high-resolution	Spillover effect: difficult to capture small-scale economic activity	Data denoising, radiometric calibration, contrast adjustment
Population Distribution Data (LandScan)	Oak Ridge National Laboratory (USA)	Reflects resident population distribution; comprehensive spatial coverage	Low update frequency; insufficient resolution	Filling missing values, standardization, resolution adjustment
Heatmap Data	Baidu Maps Open Platform	Reflects real-time population mobility hotspots	Biased toward high-mobility areas, limited by the data platform	Outlier removal, data interpolation, spatial overlay, and temporal alignment

2.2.1. NTL Data

The NPP-VIIRS (Suomi National Polar-Orbiting Partnership Visible Infrared Imaging Radiometer Suite) data, jointly provided by NASA and NOAA, has a spatial resolution of 500 m, enabling more precise capture of light intensity distributions within urban agglomerations, particularly in areas with concentrated economic activity and population density. Available since 2011, these data have a daily revisit cycle. The dynamic range of NPP-VIIRS NTL data is extensive, effectively detecting weak light sources and providing insights into economic activities in smaller and emerging cities, thus enhancing the accuracy of urban agglomeration spatial structure identification [64]. In this study, we access 2023 NPP-VIIRS NTL data for the PRD urban agglomeration through NASA's Earth Observing System Data and Information System (EOSDIS) website. The data undergo preprocessing, including cloud removal, radiance correction, and contrast adjustment, resulting in the preprocessed NTL data (Figure 2).
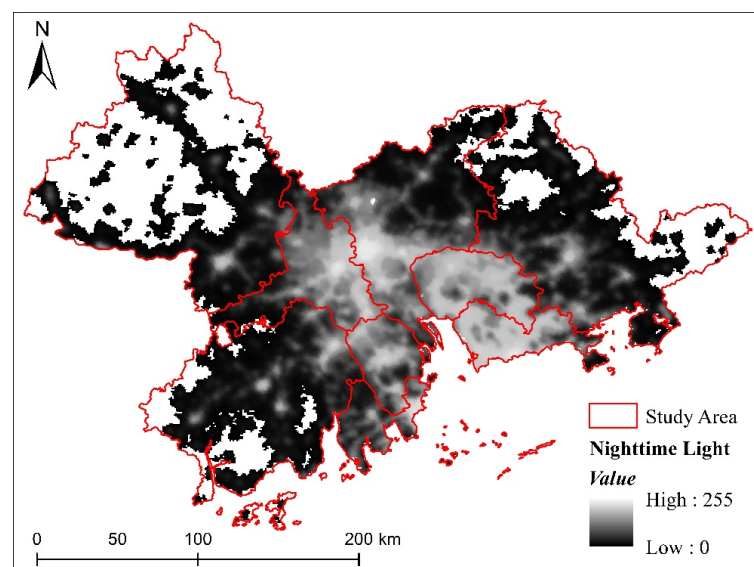

Figure 2. Preprocessed NTL Data for the PRD Urban Agglomeration.

2.2.2. LandScan Data

LandScan is a global high-resolution population distribution dataset developed by the Oak Ridge National Laboratory in the United States. It is generated using a combination of remote sensing, census data, and geographic information, producing a global population distribution map with a resolution of 30 arc seconds (approximately 1 km). This dataset is widely applied for analyzing global population spatial dynamics. Compared to traditional population data, LandScan's advantage lies in its high spatial resolution and ability to capture both daytime and nighttime population activities, making it particularly suitable for studies within the spatial structure of urban agglomerations [65]. In this study, we obtain 2023 population distribution data for the PRD urban agglomeration from the official website (https://landscan.ornl.gov/, accessed on 10 November 2024). We preprocess the data by filling in missing values, normalizing population density, and adjusting spatial resolution, resulting in the preprocessed LandScan data (Figure 3).
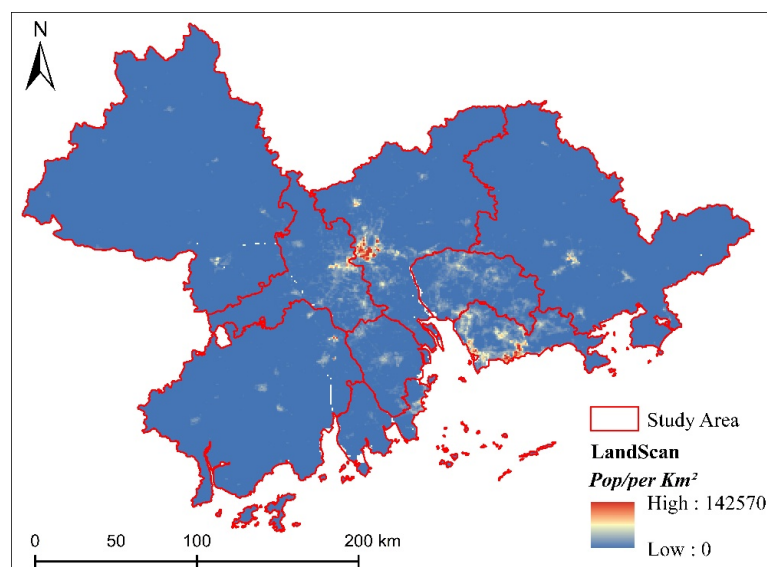
Figure 3. Preprocessed LandScan Data for the PRD Urban Agglomeration.

2.2.3. Heatmap Data

Population mobility refers to the migration and movement of people between different regions for reasons such as employment, education, and housing. It reveals the strength of connections between regions, the intensity of socio-economic activities, and the balance of resource distribution. In population mobility studies, heatmaps are a commonly used visualization tool, representing the density of certain phenomena in space through color gradients. Specifically, in population mobility research, heatmaps can illustrate high- and low-density migration areas, highlighting hotspots of population concentration within a specific timeframe and their changing trends. Compared to other forms of data representation, such as traditional point or line charts, heatmaps provide a more intuitive view of hotspots and spatial distribution patterns of population mobility, aiding in identifying regional activity levels and population aggregation trends [66].

Numerous platforms provide heatmap data, such as Baidu Maps, Google Maps, and Tencent Maps. Among them, Baidu Maps, with its large user base, extensive coverage, and high-precision location information, offers real-time updates and API support on an open platform, making its heatmap data widely utilized for analyzing patterns of population concentration and movement within cities. In this study, we obtain 2023 heatmap data for the PRD urban agglomeration through Baidu Maps' open platform website (https://lbsyun.baidu.com/, accessed on 15 November 2024). To enhance data accuracy and effectiveness, we perform rigorous data cleaning and preprocessing. The specific steps included: first, removing outliers and noise, such as missing data or inaccurate geographic coordinates; second, resampling and interpolating the data to address inconsistencies in temporal and spatial resolution due to uneven data collection frequencies; finally, conducting spatial overlay and temporal alignment to produce the preprocessed heatmap data (Figure 4).
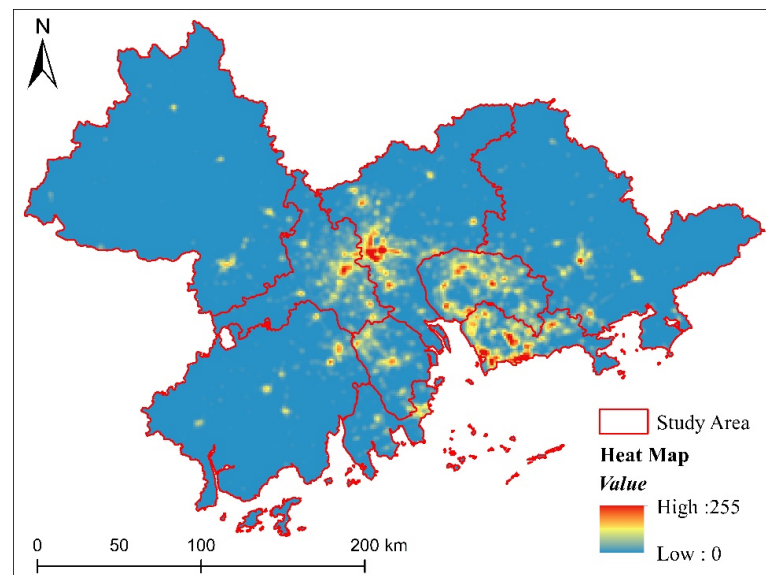
Figure 4. Preprocessed Heatmap Data of the PRD Urban Agglomeration.

2.3. Methods

2.3.1. Wavelet Transform

Wavelet Transform (WT) is an algorithm that effectively integrates different signals by decomposing them into various frequency components for analysis. Unlike the Fourier Transform, the Wavelet Transform possesses time-frequency localization properties, allowing for localized analysis in both the time and frequency domains. This enables the Wavelet Transform to observe global trends and local details at multiple scales, making it particularly suitable for analyzing and identifying the spatial range of urban agglomerations [67]. We choose wavelet transform as the data fusion method because of its powerful multi-scale analysis capability. Through wavelet decomposition, features from different data sources, such as the brightness distribution of NTL data and the hotspot distribution of population mobility data, can be extracted at multiple levels and fused with high quality through inverse transformation. This method effectively captures the economic and population dynamics within the Pearl River Delta region and shows strong applicability, especially in high-activity areas like the Guangzhou–Shenzhen corridor [67].

The process of using Wavelet Transform for data fusion involves the following steps: First, each dataset undergoes multi-scale wavelet decomposition, breaking down the original data into detail coefficients and approximation coefficients at different scales to extract multi-level features. Next, according to a predefined fusion strategy (e.g., weighted averaging, selecting maximum values), feature extraction and fusion processing are performed on the decomposition coefficients across each frequency band to retain key informational features during fusion [68]. Finally, by applying the inverse wavelet transform, the fused frequency band coefficients are reconstructed back into the original space, resulting in a new dataset that integrates both brightness information and population distribution features, thereby producing higher-quality composite data. The formula for Wavelet Transform is as follows:

$$WT(\alpha, \tau) = f(t)\varphi(t) = \frac{1}{\sqrt{\alpha}} f(t) \int\limits_{-\infty}^{+\infty} \varphi(\frac{t-b}{\alpha}) dt \tag{1}$$

where $f(t)$ is the image signal vector, $\varphi(t)$ is the wavelet transform function, α is the wavelet transform scale, τ is the translation of the image signal, and b is a parameter.

2.3.2. SegNet Neural Network

SegNet is a deep convolutional neural network architecture widely used in remote sensing image analysis. Its structure consists of an encoder and a decoder; the encoder progressively extracts image features through convolution and pooling layers, while the decoder up-samples by using pooling indices, effectively restoring spatial resolution [69]. Compared to traditional deconvolution methods, SegNet's upsampling process is more lightweight and precise, enabling it to maintain computational efficiency while accurately reconstructing image details. This makes it particularly suitable for segmenting urban parcels in large-scale remote sensing images. In identifying urban spatial boundaries, SegNet is trained on annotated data, using a cross-entropy loss function to optimize the model, allowing it to distinguish urban areas from non-urban regions. After predicting new remote sensing images with the trained model, threshold processing is applied to generate binary images, followed by denoising and smoothing of the results. This allows for quantitative analysis of urban spatial range, supporting studies on urban expansion and spatial layout [70]. Overall, SegNet, as a deep convolutional neural network model, demonstrates significant advantages in processing large-scale remote sensing imagery. Compared to traditional methods, SegNet preserves pooling indices, enabling efficient feature extraction while accurately restoring the spatial resolution of images. Given the multi-centered and complex characteristics of the Pearl River Delta urban agglomeration, SegNet efficiently identifies core cities and peripheral functional zones, providing stronger support for the dynamic identification of spatial ranges [71]. The formula for SegNet is as follows.

Encoder Part:

$$Z^{(l)} = f(W^{(l)} * X + b^{(l)}) \tag{2}$$

where $Z^{(l)}$ is the feature map of the l-th layer, $W^{(l)}$ is the convolution kernel of the l-th layer, $*$ is the convolution operation, $b^{(l)}$ is the bias term of the l-th layer, and f is the nonlinear activation function.

$$P^{(l)} = MaxPool(Z^{(l)}) \tag{3}$$

Here, $P^{(l)}$ is the pooled feature map.

Decoder Part:

$$Z'^{(l)} = Unpool(P^{(l)}, pooling\ indices) \tag{4}$$

where $Z'^{(l)}$ is the up-sampling result at the l-th layer. The up-sampled feature map is smoothed and refined through convolution:

$$X'^{(l)} = W'^{(l)} * Z'^{(l)} + b'^{(l)} \tag{5}$$

Final Output:

$$\hat{y}_i = Softmax(X'^{(l)}) \tag{6}$$

Here, $\hat{y}_i$ is the predicted class for pixel i, and l is the final layer.

In urban spatial range identification tasks, SegNet uses high-resolution remote sensing images as input data, covering large-scale urban areas with each pixel labeled (e.g., buildings, roads, green spaces). These data are fed into the SegNet model, where the encoder extracts deep-level features through convolution and pooling operations, simultaneously reducing spatial resolution. The decoder then uses saved pooling indices for up-sampling to restore the image resolution. After training, the model can generate pixel-level segmentation maps from remote sensing images, precisely extracting areas of buildings, streets, and other urban infrastructure. This enables analysis of urban spatial layout and expansion characteristics.

2.3.3. Accuracy Validation

To evaluate the accuracy of the NTL_LandScan and NTL_Heatmap data in identifying the spatial range of the PRD urban agglomeration, we conduct verification and analysis of the urban spatial identification results by randomly selecting validation points. The spatial identification results are assessed using a confusion matrix, which allows for an accuracy evaluation by comparing the actual values of the random verification points with the identification results [72]. The evaluation methods include overall accuracy, confusion matrix, and Kappa coefficient. The confusion matrix lists classification results for each category, assisting in analyzing model performance and identifying categories that are easily confused. The results of the confusion matrix can be displayed in a two-dimensional table to show classification accuracy and error distribution across categories. The Kappa coefficient is a measure of classification consistency, excluding consistency due to random factors to more scientifically reflect the accuracy of the identification results. Based on previous studies, a typical validation sample size for urban agglomerations is 3000 random pixels; we create 3000 random validation points within the PRD area using ArcGIS. This sample size design covers different areas of the Pearl River Delta urban agglomeration, including core cities (such as Guangzhou and Shenzhen), secondary cities (such as Dongguan and Foshan), and peripheral cities (such as Jiangmen and Zhaoqing). In particular, it reflects varying intensities of economic activities and population mobility. Additionally, the design of 3000 random points follows validation methods used in existing studies on urban agglomerations of similar scales. This approach ensures statistical significance while avoiding increased computational costs caused by excessive sample sizes. Finally, this sample size aligns with mainstream practices in accuracy validation at the regional scale in existing research, providing both practicality and reliability. The formula is as follows:

$$k = \frac{p_o - p_e}{1 - p_e} \tag{7}$$

$$p_e = \frac{a_1 \times b_1 + a_2 \times b_2 + \ldots\ldots a_i \times b_i}{n \times n} \tag{8}$$

where: p_o is the overall accuracy, a is the real sample number of each category, b is the predicted sample number of each category, and n is the total sample number. By comparing the actual values of random validation points with the predicted results, the method's reliability in identifying urban boundaries can be scientifically evaluated.

3. Results

3.1. Spatial Range of the PRD Urban Agglomeration Identified by NTL_LandScan (NTL_LS) Fusion Data

The fusion of NTL data with LandScan data resulted in the NTL_LS dataset (Figure 5). The figure indicates that high-value areas of NTL_LS are primarily concentrated in the core cities of the PRD urban agglomeration, including Guangzhou, Shenzhen, and Foshan, reflecting active economic activities and high population density in these cities. Additionally, the continuous brightness distribution along the Guangzhou–Shenzhen corridor demonstrates a significant economic and population clustering effect. Secondary high-value areas include Dongguan and Zhongshan, which exhibit strong economic connections and relatively high population density, indicating that they play a secondary core role within the PRD urban agglomeration. Low-value areas are mainly located in peripheral cities such as Jiangmen, Zhaoqing, and Huizhou, suggesting relatively weaker economic activities and lower population concentration in these regions. Furthermore, high-value distributions are sparse in the northern and western regions of the PRD urban agglomeration, such as parts of Zhaoqing and Qingyuan, reflecting lower economic and population densities.
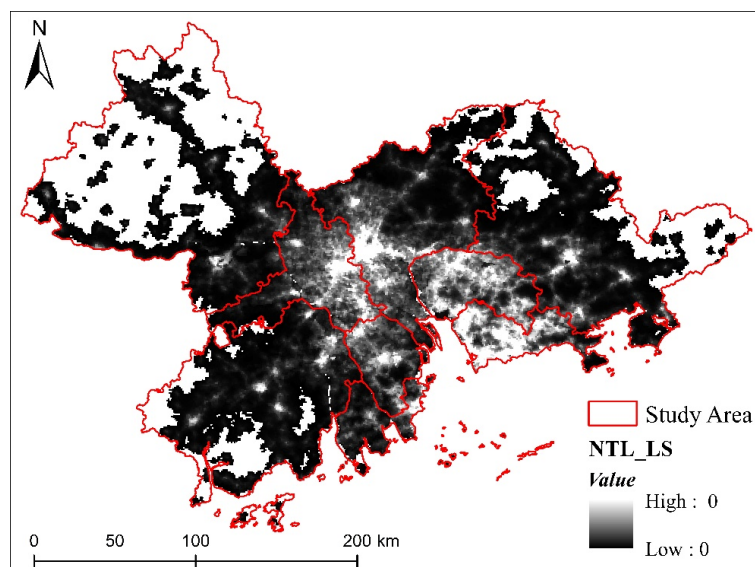
Figure 5. Fusion of NTL Data with LandScan Data.

The spatial range of the PRD urban agglomeration identified by the NTL_LS data is shown in Figure 6, with a total identified area of 6069.51 km², primarily concentrated in the central and eastern parts of the study area, including Guangzhou, Shenzhen, Foshan, and Dongguan. These cities serve as economic centers of the PRD urban agglomeration, characterized by a developed industrial base, a highly dense population, and strong resource-attracting capacity. The high brightness and population density in these areas reflect active economic activities and strong agglomeration effects. This spatial clustering is attributed to the economic advantages, industrial clusters, and well-developed urban infrastructure in these cities, which attract substantial employment opportunities and a mobile population, further driving the growth of surrounding areas.
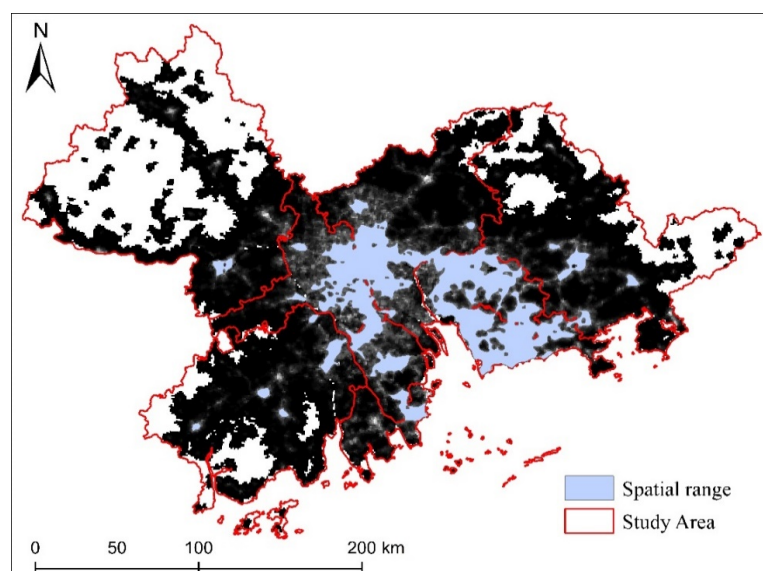

Figure 6. Spatial Range of the PRD Urban Agglomeration Identified by NTL_LS Data.

In the mid-eastern cities of the PRD urban agglomeration, such as Dongguan and Foshan, the proximity to core cities, coupled with relatively high economic and population densities, creates tight economic connections and an integrated urban network with Guangzhou and Shenzhen, establishing these cities as essential components of the PRD

urban agglomeration. This network effect reinforces spatial clustering within the region, forming a multi-core structure within the urban agglomeration. In contrast, the western and peripheral regions of the PRD urban agglomeration, including Jiangmen, Zhaoqing, and Huizhou, while encompassed within the agglomeration's spatial boundaries, exhibit lower economic and population densities, resulting in less spatial coverage identified in the NTL_LS data. This characteristic may be influenced by factors such as regional industrial structure, infrastructure development levels, and the strength of economic connections with core cities. Geographic distance and transportation accessibility further contribute to the relatively weak spatial clustering of these peripheral cities. Notably, ecological protection zones in the western PRD urban agglomeration, including wetlands and mountainous areas, also constrain spatial development in this region, impacting the spatial expansiveness of the urban agglomeration.

3.2. Spatial Range of the PRD Urban Agglomeration Identified by NTL_Heatmap (NTL_HM) Fusion Data

The NTL_HM data, generated by fusing NTL data with heatmap data, are shown in Figure 7. The high-brightness areas are primarily concentrated in core cities such as Guangzhou, Shenzhen, Foshan, and Dongguan and their surroundings; Zhongshan, Huizhou, and Zhuhai also display relatively high brightness, though lower than Guangzhou and Shenzhen. In contrast, Jiangmen and Zhaoqing exhibit significantly lower brightness, reflecting weaker economic activity and population mobility in these peripheral cities. Compared to the NTL_LS data, the high-brightness areas in the NTL_HM data more prominently represent the distribution characteristics of population mobility. The continuity of high brightness along the Guangzhou–Shenzhen corridor, in particular, highlights this corridor as not only an economic axis but also a primary channel for population movement. Zhongshan, Huizhou, and Zhuhai show relatively high brightness but lower than Guangzhou and Shenzhen, indicating weaker population mobility. This data fusion approach is more effective for analyzing the spatial patterns of economic activity and population mobility within the region.
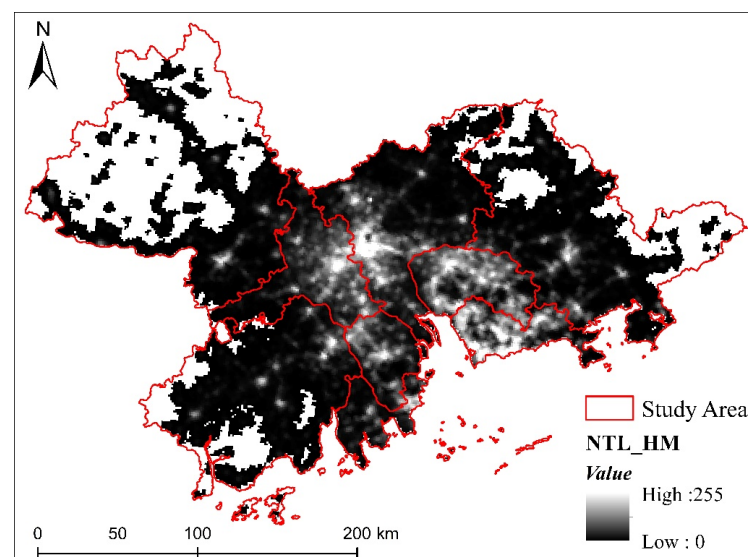

Figure 7. Fusion of NTL Data with Heatmap Data.

The spatial range of the PRD urban agglomeration identified based on NTL_HM data is widely distributed (Figure 8), covering an area of 9038.47 km^2, particularly concentrated in cities around the Pearl River Estuary, including Guangzhou, Shenzhen, Foshan, and Dongguan. These areas, marked by economic vitality and high levels of urbanization,

serve as major zones for economic activity and population mobility, reflecting the high concentration of economic and population flows within the PRD urban agglomeration. These cities, as crucial regions for economic development and population concentration, not only play a dominant role in the regional economy but also attract a significant amount of migrant population, providing employment and living opportunities for surrounding areas. Substantial spatial range is also identified in Zhongshan, Huizhou, and Zhuhai, indicating relatively high economic activity and population mobility in these regions. In particular, areas between Zhongshan, Dongguan, and Huizhou near Shenzhen show dense population flows, reflecting close economic ties with cities like Guangzhou and Shenzhen and indicating strong development potential. In contrast, the peripheral areas of the PRD urban agglomeration, such as Jiangmen and Zhaoqing, show a relatively smaller identified spatial range, suggesting lower levels of economic activity and population mobility. Due to their greater distance from the main economic centers, these cities experience a weaker economic spillover effect and thus lack the large-scale population mobility and economic agglomeration seen in core areas, placing them in regions of lower population and economic density within the PRD urban agglomeration.
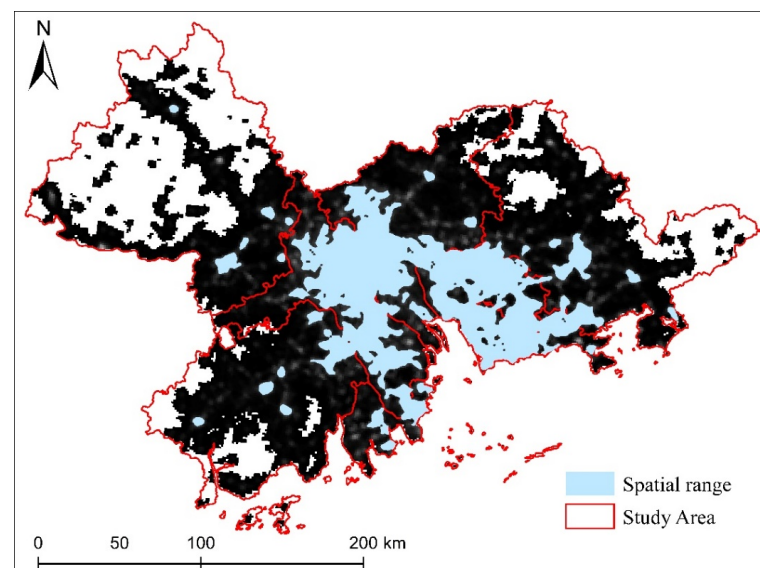

Figure 8. Spatial Range of the PRD Urban Agglomeration Identified by NTL_HM Data.

Compared to the spatial range of the PRD urban agglomeration identified by NTL_LS data, which integrates LandScan's resident population distribution characteristics, the NTL_LS-identified range emphasizes areas of stable, long-term economic activity and high population density. Consequently, it primarily captures the core areas of high economic and population concentration within the PRD urban agglomeration. By contrasting the spatial range identified by the two datasets, it becomes apparent that cities like Guangzhou and Shenzhen have the highest resident population density and most active economic activity, while areas such as Zhongshan, Huizhou, and Zhuhai exhibit relatively less economic and population mobility, resulting in a smaller identified range. Peripheral cities like Jiangmen and Zhaoqing display even smaller spatial ranges, with lower levels of economic activity and fewer residents, indicating that these areas are in a low-density state regarding resident population and economic agglomeration within the PRD urban agglomeration.

3.3. Comparative Analysis

Based on the fusion results of NTL data with LandScan and heatmap data, respectively, the NTL-fused heatmap data demonstrate higher accuracy and consistency in identifying

the spatial range of the PRD urban agglomeration (Table 2). Specifically, the identification accuracy of NTL_HM reaches 89.17%, compared to 80.37% for NTL_LS. Additionally, the Kappa coefficient for NTL_HM is 0.7342, significantly higher than the 0.5225 for NTL_LS. The Kappa coefficient measures the consistency of classification results, with higher values indicating more reliable classifications. Therefore, in terms of accuracy and consistency, NTL_HM clearly outperforms NTL_LS in identifying the range of the PRD urban agglomeration.

Table 2. Verification of Identification Results.

Data		Urban	Rural	Accuracy	Kappa
NTL_LS	Urban	1794	353	80.37%	0.5225
	Rural	236	617		
NTL_HM	Urban	1978	169	89.17%	0.7342
	Rural	156	697		

The advantage of NTL_HM in identification lies primarily in its capacity to capture dynamic population mobility and its high adaptability to economic activity levels. The dynamic population mobility information provided by heatmap data compensates for the limitation of LandScan data, which only represent resident population density. This enables NTL_HM to more accurately identify areas of frequent economic activity and population mobility within the PRD urban agglomeration, particularly in transition zones and expansion areas between cities. Specifically, compared to NTL_LS data, NTL_HM data capture a wider spatial range due to their high sensitivity to dynamic population mobility. For example, in the Guangzhou–Shenzhen corridor and cities along both sides of the Pearl River Estuary, the NTL_HM method identifies a broader range, as these areas experience frequent population mobility and active economic activities. In contrast, the NTL_LS method, which relies on resident population distribution, focuses more on core urban areas and overlooks the mobility characteristics of secondary cities and transitional zones. This difference highlights the unique advantage of dynamic data in identifying spatial ranges. Therefore, with its sensitivity to economically active zones and population mobility characteristics, NTL_HM is better suited for identifying fast-growing and highly dynamic urban agglomerations like the PRD urban agglomeration. In contrast, due to its reliance on resident population distribution, NTL_LS data respond less effectively to dynamic economic and population characteristics, resulting in relatively limited spatial range identification for peripheral areas and secondary cities.

Overall, NTL_HM data demonstrate higher accuracy and consistency in identifying the spatial range of the PRD urban agglomeration, confirming the importance and effectiveness of dynamic population mobility information in urban agglomeration spatial identification.

4. Discussion

This study identifies the spatial range of the PRD urban agglomeration by fusing NTL data, Landscan residential population data, and heatmap data on the floating population. By combining the static distribution of the resident population with the dynamic characteristics of the floating population, this approach aims to overcome the limitations of traditional methods that rely solely on resident population or economic activity data. Data on the floating population capture the characteristics of short-term economic activities and dynamic changes in population mobility, which traditional methods relying on resident population data cannot reflect [73]. Observing high-mobility patterns in areas such as the Guangzhou–Shenzhen corridor, Dongguan, and Foshan reveals dynamic changes in economic functional zones and sub-core areas within the Pearl River Delta. Furthermore,

this method plays a significant role in analyzing cross-regional functional networks, such as logistics corridors and transportation hubs, and offers new research directions for the dynamic adjustment of urban agglomeration boundaries in the future [74]. The integrated identification process with multi-source data not only delineates the spatial boundaries of the PRD urban agglomeration but also highlights dynamic hotspots of population movement within the region. This approach provides a scientific basis and reference for accurately defining the spatial range of the PRD urban agglomeration.

Introducing floating population data into the identification of urban agglomeration spatial range is of significant importance [26]. Traditional studies often rely on census data of the resident population or single-source economic activity data, which, while reflecting the long-term aggregation characteristics of urban agglomerations, fail to capture short-term economic and population dynamics. This limitation constrains the identification of urban agglomeration spatial range to a static model [75,76]. Some studies have analyzed the spatial expansion of the PRD or other regional urban agglomerations through census or economic statistical data; however, these methods have limitations in identifying high-mobility areas and primarily reflect the stable core regions of economic and population concentration [77,78]. Consequently, the boundaries of urban agglomerations tend to remain fixed, overlooking the identification of active economic corridors and high-mobility zones within the region [79]. In contrast, this study fuses the mobility characteristics reflected by heatmap data, enabling the identification results to encompass not only areas of stable population aggregation but also non-central urban areas with high economic activity and dense population movement. Consequently, the identified spatial range offers a more comprehensive representation of the expansion areas surrounding cities. Comparative analysis reveals that the spatial range identified by our NTL_HM data is broader, as urban agglomeration boundaries are inherently dynamic [80]. For example, the identified Guangzhou–Shenzhen corridor and its extended areas better capture the active elements within the PRD urban agglomeration compared to traditional methods. Conventional approaches based on resident population or economic activity often overlook or marginalize these high-mobility areas [18,81], resulting in a relatively smaller, more fixed boundary [82]. In contrast, the NTL_HM data in this study, by incorporating dynamic data, more accurately reflects the actual dynamic expansion of urban agglomerations. Therefore, our findings differ from traditional identification methods in some ways, yet they offer a distinct advantage in recognizing high-mobility areas, underscoring the importance of floating population data in identifying dynamic spatial range.

This study proposes a dynamic identification method based on multi-source data fusion, combining NTL data with static resident population data and dynamic floating population data to enhance the accuracy and applicability of identifying the spatial range of the PRD urban agglomeration. This approach effectively addresses the limitations of relying on single-source data, revealing both the stable economic and population aggregation areas of the PRD and identifying hotspots of economic activity and population mobility. It offers a new approach to urban agglomeration spatial identification that integrates dynamic and static factors. Furthermore, this integrated method provides a more scientific basis for regional planning and policymaking, especially in highly economically active regions like the PRD, underscoring its strong practical value. The results of this study hold significant implications for regional policy planning. The edge cities identified through the NTL_HM method, such as Jiangmen and Zhaoqing, show lower economic activity intensity but higher population mobility density. This indicates their potential for growth within the regional economic network. Policymakers can gradually enhance the economic connectivity of these regions to the core cities by strengthening infrastructure development and industrial support policies in these regions, thereby realizing the bal-

anced development of the PRD region. Additionally, the identified high-mobility areas, such as the Guangzhou–Shenzhen corridor, can serve as priority regions for optimizing transportation hubs and public resource allocation. Specifically, in transportation planning, the population mobility hotspots identified by heatmap data provide a key basis for optimizing the layout of regional transportation hubs. By building efficient transportation networks, these efforts promote the rational flow of resources and labor within the urban agglomeration. In terms of public service allocation, identifying high-mobility and sub-core areas allows the government to more precisely allocate public resources such as healthcare and education, alleviating overcrowding in core cities. In economic planning, the dynamic population mobility trends observed in edge cities, such as Zhaoqing and Jiangmen, offer new directions for promoting regional economic integration. Relevant departments can formulate industrial policies targeting these areas to help them gradually integrate into the Pearl River Delta urban agglomeration network.

However, this study has certain limitations, primarily in capturing spatiotemporal dynamics. Due to the limited time span and granularity of the data, this study is unable to explore in depth the dynamic impacts of population mobility on the urban agglomeration boundary across different time periods [83]. Additionally, there is a degree of ambiguity in identifying peripheral areas, which may lead to an underestimation of regions with low economic activity but high mobility [84]. Therefore, future research could enhance the capacity for dynamic monitoring of spatiotemporal changes in urban agglomerations by incorporating finer time scales and more diverse dynamic data sources (such as traffic flow and social media data). This would allow for a more accurate reflection of the spatiotemporal evolution patterns of urban agglomerations, providing a more precise basis for spatial range identification and future development predictions.

5. Conclusions

This study fuses NTL data, resident population data, and floating population data to identify the spatial range of the PRD urban agglomeration from the dual perspectives of population distribution and population mobility. The results show that the spatial range identified by NTL_LS covers 6069.51 km^2, with an accuracy of 80.37% and a Kappa coefficient of 0.5225, whereas the spatial range identified by NTL_HM covers 90,338.47 km^2, with an accuracy of 89.17% and a Kappa coefficient of 0.7342. The accuracy and consistency of NTL_HM are significantly higher than those of NTL_LS. The NTL_HM-identified spatial range of the PRD is broader, particularly in the Guangzhou–Shenzhen corridor and its surrounding expansion areas, offering more comprehensive coverage of high-mobility zones and short-term economic activity hotspots. This suggests that incorporating floating population data into urban agglomeration identification not only improves the accuracy of spatial range identification but also better reflects the dynamic characteristics of population and economic activity in economically active regions like the PRD. This approach effectively addresses the limitations of resident population data in capturing economic and population dynamics.

This study provides a new approach for urban agglomeration spatial range identification based on multi-source data integration by comparing the identification results of NTL_HM and NTL_LS data. By incorporating the dynamic characteristics of economic activity and population mobility, the identification method proposed in this study not only enhances the accuracy of spatial range identification but also offers more timely and dynamic reference information for regional planning and policymaking in complex urban agglomerations like the PRD urban agglomeration.

References

1. Luo, Q.; Cui, R.; Zhao, X. Impact of Productive Service Agglomeration on Urban Technological Innovation: Based on China's 19 Urban Agglomerations. *J. Urban Plan. Dev.* **2024**, *150*, 04024045. [CrossRef]

2. Fang, C.; Yu, D. Urban agglomeration: An evolving concept of an emerging phenomenon. *Landsc. Urban Plan.* **2017**, *162*, 126–136. [CrossRef]

3. Yu, Q.; Li, M.; Li, Q.; Wang, Y.; Chen, W. Economic agglomeration and emissions reduction: Does high agglomeration in China's urban clusters lead to higher carbon intensity? *Urban Clim.* **2022**, *43*, 101174. [CrossRef]

4. Sun, J.; Zhai, N.; Mu, H.; Miao, J.; Li, W.; Li, M. Assessment of urban resilience and subsystem coupling coordination in the Beijing-Tianjin-Hebei urban agglomeration. *Sustain. Cities Soc.* **2024**, *100*, 105058. [CrossRef]

5. Huang, Y.; Hong, T.; Ma, T. Urban network externalities, agglomeration economies and urban economic growth. *Cities* **2020**, *107*, 102882. [CrossRef]

6. Zeng, C.; Song, Y.; Cai, D.; Hu, P.; Cui, H.; Yang, J.; Zhang, H. Exploration on the spatial spillover effect of infrastructure network on urbanization: A case study in Wuhan urban agglomeration. *Sustain. Cities Soc.* **2019**, *47*, 101476. [CrossRef]

7. Balsa-Barreiro, J.; Li, Y.; Morales, A. Globalization and the shifting centers of gravity of world's human dynamics: Implications for sustainability. *J. Clean. Prod.* **2019**, *239*, 117923. [CrossRef]

8. Zhang, S.; Wei, H. Identification of Urban Agglomeration Spatial Range Based on Social and Remote-Sensing Data—For Evaluating Development Level of Urban Agglomeration. *ISPRS Int. J. Geo-Inf.* **2022**, *11*, 456. [CrossRef]

9. Cao, Y.; Zhang, R.; Zhang, D.; Zhou, C. Urban agglomerations in China: Characteristics and influencing factors of population agglomeration. *Chin. Geogr. Sci.* **2023**, *33*, 719–735. [CrossRef]

10. Wei, G.; Li, X.; Yu, M.; Lu, G.; Chen, Z. Influence mechanism of transportation integration on industrial agglomeration in urban agglomeration theory—Taking the Yangtze River Delta urban agglomeration as an example. *Appl. Sci.* **2022**, *12*, 8369. [CrossRef]

11. Zornoza-Gallego, C. Means of Transport and Population Distribution in Metropolitan Areas: An Evolutionary Analysis of the Valencia Metropolitan Area. *Land* **2022**, *11*, 657. [CrossRef]

12. Busłowska, A.; Marcinkiewicz, J. Social cohesion of functional urban areas (Example of Eastern Poland). *Soc. Indic. Res.* **2023**, *167*, 451–473. [CrossRef]

13. Perez Martinez, M.E. Adaptability of rural dwellers and settlements in conurbation areas: The case of bogota, colombia. *Cuad. Desarro. Rural* **2008**, *5*, 61–86.

14. Manole, S.D.; Tache, A.V.; Meiţă, V.; Petrișor, A.I. Analysis of Romanian Polycentricity Based on Functional Urban Areas. *Mitteilungen Osterreichischen Geogr. Ges.* **2020**, *1*, 161–188. [CrossRef]

15. Fan, Q.; Mei, X.; Zhang, C.; Yang, X. Research on Gridding of Urban Spatial Form Based on Fractal Theory. *ISPRS Int. J. Geo-Inf.* **2022**, *11*, 622. [CrossRef]

16. Davidson, M. Situational analysis and urban theory. *Prog. Hum. Geogr.* **2024**, *48*, 113–130. [CrossRef]

17. Chettry, V.; Surawar, M. Delineating urban growth boundary using remote sensing, ANN-MLP and CA model: A case study of Thiruvananthapuram urban agglomeration, India. *J. Indian Soc. Remote Sens.* **2021**, *49*, 2437–2450. [CrossRef]

18. Oliveira, E.A.; Furtado, V.; Andrade, J.S.; Makse, H.A. A worldwide model for boundaries of urban settlements. *R. Soc. Open Sci.* **2018**, *5*, 180468. [CrossRef] [PubMed]

19. Bartolacci, F.; Salvia, R.; Quaranta, G.; Salvati, L. Seeking the Optimal Dimension of Local Administrative Units: A Reflection on Urban Concentration and Changes in Municipal Size. *Sustainability* **2022**, *14*, 15240. [CrossRef]

20. Ma, H.; Xu, X. Knowledge polycentricity of China's urban agglomerations. *J. Urban Plan. Dev.* **2022**, *148*, 04022014. [CrossRef]

21. Yin, H.; Xiao, R.; Fei, X.; Zhang, Z.; Gao, Z.; Wan, Y.; Guo, Y. Analyzing "economy-society-environment" sustainability from the perspective of urban spatial structure: A case study of the Yangtze River delta urban agglomeration. *Sustain. Cities Soc.* **2023**, *96*, 104691. [CrossRef]

22. Ahmad, M.; Jabeen, G. Dynamic causality among urban agglomeration, electricity consumption, construction industry, and economic performance: Generalized method of moments approach. *Environ. Sci. Pollut. Res.* **2020**, *27*, 2374–2385. [CrossRef] [PubMed]

23. Yu, X.; Wu, Z.; Zheng, H.; Li, M.; Tan, T. How urban agglomeration improve the emission efficiency? A spatial econometric analysis of the Yangtze River Delta urban agglomeration in China. *J. Environ. Manag.* **2020**, *260*, 110061. [CrossRef] [PubMed]

24. He, X.; Yuan, X.; Zhang, D.; Zhang, R.; Li, M.; Zhou, C. Delineation of urban agglomeration boundary based on multisource big data fusion—A case study of Guangdong–Hong Kong–Macao Greater Bay Area (GBA). *Remote Sens.* **2021**, *13*, 1801. [CrossRef]

25. Peng, J.; Lin, H.; Chen, Y.; Blaschke, T.; Luo, L.; Xu, Z.; Wu, J. Spatiotemporal evolution of urban agglomerations in China during 2000–2012: A nighttime light approach. *Landsc. Ecol.* **2020**, *35*, 421–434. [CrossRef]

26. Wang, X.; Ding, S.; Cao, W.; Fan, D.; Tang, B. Research on network patterns and influencing factors of population flow and migration in the Yangtze River Delta urban agglomeration, China. *Sustainability* **2020**, *12*, 6803. [CrossRef]

27. Smith, D.A. Visualising world population density as an interactive multi-scale map using the global human settlement population layer. *J. Maps* **2017**, *13*, 117–123. [CrossRef]

28. Klotz, M.; Kemper, T.; Geiß, C.; Esch, T.; Taubenböck, H. How good is the map? A multi-scale cross-comparison framework for global settlement layers: Evidence from Central Europe. *Remote Sens. Environ.* **2016**, *178*, 191–212. [CrossRef]

29. Bhatta, B. Modelling of urban growth boundary using geoinformatics. *Int. J. Digit. Earth* **2009**, *2*, 359–381. [CrossRef]

30. Fang, C. Important progress and future direction of studies on China's urban agglomerations. *J. Geogr. Sci.* **2015**, *25*, 1003–1024. [CrossRef]

31. Ren, T.; Huang, H.J.; Nie, Y.M. High-speed rail in China: Implications for intercity commuting and urban spatial structure. *Sustain. Cities Soc.* **2023**, *97*, 104719. [CrossRef]

32. Cheng, Y.; Zheng, D. Does the Digital Economy Promote Coordinated Urban–Rural Development? Evidence from China. *Sustainability* **2023**, *15*, 5460. [CrossRef]

33. Wang, F.; Wang, G.; Liu, J.; Chen, H. How does urbanization affect carbon emission intensity under a hierarchical nesting structure? Empirical research on the China Yangtze River Delta urban agglomeration. *Environ. Sci. Pollut. Res.* **2019**, *26*, 31770–31785. [CrossRef]

34. Liu, R.; Dong, X.; Wang, X.C.; Zhang, P.; Liu, M.; Zhang, Y. Study on the relationship among the urbanization process, ecosystem services and human well-being in an arid region in the context of carbon flow: Taking the Manas river basin as an example. *Ecol. Indic.* **2021**, *132*, 108248. [CrossRef]

35. He, X.; Zhu, Y.; Chang, P.; Zhou, C. Using tencent user location data to modify night-time light data for delineating urban agglomeration boundaries. *Front. Environ. Sci.* **2022**, *10*, 860365. [CrossRef]

36. Liu, W.; Liu, D.; Liu, Y. Spatially heterogeneous response of carbon storage to land use changes in Pearl River Delta urban agglomeration, China. *Chin. Geogr. Sci.* **2023**, *33*, 271–286. [CrossRef]

37. Song, Y.; Li, X.; Tao, G.; Liu, J. Exploring the Characteristics and Drivers of Expansion in the Shandong Peninsula Urban Agglomeration Based on Nighttime Light (NTL) Data. *IEEE J. Sel. Top. Appl. Earth Obs. Remote Sens.* **2023**, *16*, 8535–8549. [CrossRef]

38. Shi, K.; Wu, Y.; Liu, S.; Chen, Z.; Huang, C.; Cui, Y. Mapping and evaluating global urban entities (2000–2020): A novel perspective to delineate urban entities based on consistent nighttime light data. *GISci. Remote Sens.* **2023**, *60*, 2161199. [CrossRef]

39. Zhang, L.; Fang, C.; Zhao, R.; Zhu, C.; Guan, J. Spatial–temporal evolution and driving force analysis of eco-quality in urban agglomerations in China. *Sci. Total Environ.* **2023**, *866*, 161465. [CrossRef] [PubMed]

40. Tordoir, P.P.; van Raan, A.F.; Poorthuis, A. Effects of municipal boundaries measured by combining urban scaling and spatial interaction. *J. R. Soc. Interface* **2023**, *20*, 20220775. [CrossRef]

41. Shen, Z.; Xu, X.; Sun, Z.; Jiang, Y.; Shi, H. Regional thermal environments (RTEs) and driving forces in six urban agglomerations of China and America. *Build. Environ.* **2023**, *235*, 110185. [CrossRef]

42. Zeng, P.; Zong, C. Research on the relationship between population distribution pattern and urban industrial facility agglomeration in China. *Sci. Rep.* **2023**, *13*, 16225. [CrossRef] [PubMed]

43. Wu, H.; Wang, L.; Zhang, Z.; Gao, J. Analysis and optimization of 15-minute community life circle based on supply and demand matching: A case study of Shanghai. *PLoS ONE* **2021**, *16*, e0256904. [CrossRef]

44. Sun, S.; Xie, Y.; Li, Y.; Yuan, K.; Hu, L. Analysis of dynamic evolution and spatial-temporal heterogeneity of carbon emissions at county level along "the belt and road"—A case study of northwest China. *Int. J. Environ. Res. Public Health* **2022**, *19*, 13405. [CrossRef]

45. Zhou, Y.; He, X.; Zhu, Y. Identification and evaluation of the polycentric urban structure: An empirical analysis based on multi-source big data fusion. *Remote Sens.* **2022**, *14*, 2705. [CrossRef]

46. Rao, D.K.; Chandrasekharam, D. Quantifying the water footprint of an urban agglomeration in developing economy. *Sustain. Cities Soc.* **2019**, *50*, 101686.

47. He, X.; Zhang, R.; Yuan, X.; Cao, Y.; Zhou, C. The role of planning policy in the evolution of the spatial structure of the Guangzhou metropolitan area in China. *Cities* **2023**, *137*, 104284. [CrossRef]

48. Hattori, R.; Horie, S.; Hsu, F.C.; Elvidge, C.D.; Matsuno, Y. Estimation of in-use steel stock for civil engineering and building using nighttime light images. *Resour. Conserv. Recycl.* **2014**, *83*, 1–5. [CrossRef]

49. Zhang, Y.; Wang, H.; Luo, K.; Wu, C.; Li, S. Study on Spatialization and Spatial Pattern of Population Based on Multi-Source Data—A Case Study of the Urban Agglomeration on the North Slope of Tianshan Mountain in Xinjiang, China. *Sustainability* **2024**, *16*, 4106. [CrossRef]

50. Levin, N.; Zhang, Q. A global analysis of factors controlling VIIRS nighttime light levels from densely populated areas. *Remote Sens. Environ.* **2017**, *190*, 366–382. [CrossRef]

51. Beyer, R.C.; Franco-Bedoya, S.; Galdo, V. Examining the economic impact of COVID-19 in India through daily electricity consumption and nighttime light intensity. *World Dev.* **2021**, *140*, 105287. [CrossRef]

52. Yang, R.; Zhou, Q.; Xu, L.; Zhang, Y.; Wei, T. Forecasting the Total Output Value of Agriculture, Forestry, Animal Husbandry, and Fishery in Various Provinces of China via NPP-VIIRS Nighttime Light Data. *Appl. Sci.* **2024**, *14*, 8752. [CrossRef]

53. Chen, Y.; Wang, S.; Gu, Z.; Yang, F. Modeling the Spatial Distribution of Population Based on Random Forest and Parameter Optimization Methods: A Case Study of Sichuan, China. *Appl. Sci.* **2024**, *14*, 446. [CrossRef]

54. Wang, C.; Yin, L. Defining urban big data in urban planning: Literature review. *J. Urban Plan. Dev.* **2023**, *149*, 04022044. [CrossRef]

55. Liu, J.; Li, T.; Xie, P.; Du, S.; Teng, F.; Yang, X. Urban big data fusion based on deep learning: An overview. *Inf. Fusion* **2020**, *53*, 123–133. [CrossRef]

56. Ge, R.; Li, X.; Yuan, F.; Jowitt, S.M.; Dou, F.; Xiong, Y.; Li, X. Demand evaluation of urban underground space through geospatial big data. *J. Urban Plan. Dev.* **2024**, *150*, 04023057. [CrossRef]

57. He, X.; Zhou, Y.; Yuan, X.; Zhu, M. The coordination relationship between urban development and urban life satisfaction in Chinese cities-An empirical analysis based on multi-source data. *Cities* **2024**, *150*, 105016. [CrossRef]

58. Sainio, J.; Westerholm, J.; Oksanen, J. Generating heat maps of popular routes online from massive mobile sports tracking application data in milliseconds while respecting privacy. *ISPRS Int. J. Geo-Inf.* **2015**, *4*, 1813–1826. [CrossRef]

59. Delgado, J.; Saavedra, P. Global bifurcation diagram for the Kerner–Konhäuser traffic flow model. *Int. J. Bifurc. Chaos* **2015**, *25*, 1550064. [CrossRef]

60. Gao, X.; Xia, N.; Zhuang, S.; Zhao, X.; Liang, J.; Wang, Z.; Li, M. Integrating multi-source geographic big data to delineate urban growth boundary: A case study of Changsha. *IEEE J. Sel. Top. Appl. Earth Obs. Remote Sens.* **2024**, *17*, 9018–9036. [CrossRef]

61. Wang, K.; Ji, X.; Liu, S.; Zhu, J.; Liu, K. Harnessing big data for sustainable urban management: A novel approach to gridded urban GDP dataset development. *J. Clean. Prod.* **2024**, *444*, 141205. [CrossRef]

62. He, X.; Zhou, C.; Zhang, J.; Yuan, X. Using wavelet transforms to fuse nighttime light data and POI big data to extract urban built-up areas. *Remote Sens.* **2020**, *12*, 3887. [CrossRef]

63. He, X.; Cao, Y.; Zhou, C. Evaluation of polycentric spatial structure in the urban agglomeration of the pearl river delta (PRD) based on multi-source big data fusion. *Remote Sens.* **2021**, *13*, 3639. [CrossRef]

64. Kii, M.; Matsumoto, K.; Sugita, S. Future Scenarios of Urban Nighttime Lights: A Method for Global Cities and Its Application to Urban Expansion and Carbon Emission Estimation. *Remote Sens.* **2024**, *16*, 1018. [CrossRef]

65. He, X.; Zhou, Y. Urban spatial growth and driving mechanisms under different urban morphologies: An empirical analysis of 287 Chinese cities. *Landsc. Urban Plan.* **2024**, *248*, 105096. [CrossRef]

66. Tieskens, K.F.; Smith, I.A.; Jimenez, R.B.; Hutyra, L.R.; Fabian, M.P. Mapping the gaps between cooling benefits of urban greenspace and population heat vulnerability. *Sci. Total Environ.* **2022**, *845*, 157283. [CrossRef] [PubMed]

67. Peng, J.; Liu, Y.; Ma, J.; Zhao, S. A new approach for urban-rural fringe identification: Integrating impervious surface area and spatial continuous wavelet transform. *Landsc. Urban Plan.* **2018**, *175*, 72–79. [CrossRef]

68. Myint, S.W.; Zhu, T.; Zheng, B. A novel image classification algorithm using overcomplete wavelet transforms. *IEEE Geosci. Remote Sens. Lett.* **2015**, *12*, 1232–1236. [CrossRef]

69. Son, S.; Lee, S.H.; Bae, J.; Ryu, M.; Lee, D.; Park, S.R.; Kim, J. Land-cover-change detection with aerial orthoimagery using segnet-based semantic segmentation in Namyangju city, South Korea. *Sustainability* **2022**, *14*, 12321. [CrossRef]

70. Rastogi, K.; Bodani, P.; Sharma, S.A. Automatic building footprint extraction from very high-resolution imagery using deep learning techniques. *Geocarto Int.* **2022**, *37*, 1501–1513. [CrossRef]

71. Zhou, H.; Xu, C.; Pu, H.; Nie, Y.; Sun, J. Influence of urban surface compositions on outdoor thermal environmental parameters on an urban road: A combined two-aspect analysis. *Sustain. Cities Soc.* **2023**, *90*, 104376. [CrossRef]

72. He, X.; Zhang, Z.; Yang, Z. Extraction of urban built-up area based on the fusion of night-time light data and point of interest data. *R. Soc. Open Sci.* **2021**, *8*, 210838. [CrossRef]

73. He, J.; Chen, L.; Zhang, W. Satisfaction differences in urban features between natives and floating population: Evidence from eleven cities in China. *J. Urban Plan. Dev.* **2022**, *148*, 05022038. [CrossRef]

74. Cao, Y.; He, X.; Zhou, C. Characteristics and Influencing Factors of Population Migration under Different Population Agglomeration Patterns—A Case Study of Urban Agglomeration in China. *Sustainability* **2023**, *15*, 6909. [CrossRef]

75. Shi, S.; Liu, G. Spatial matching relationship between health tourism destinations and population aging in the Yangtze River Delta Urban Agglomeration. *Environ. Res. Commun.* **2023**, *5*, 095001. [CrossRef]

76. Bai, M.; Zhang, S.; Wang, X.; Feng, Y.; Wang, J.; Peng, P. Deep semantic segmentation for rapid extraction and spatial-temporal expansion variation analysis of China's urban built-up areas. *Front. Earth Sci.* **2022**, *10*, 883779. [CrossRef]

77. Ouyang, T.; Kuang, Y.; Hu, Z.; Sun, B. Urbanization in the pearl river delta economic zone, China. *Int. J. Sustain. Dev. World Ecol.* **2005**, *12*, 48–54. [CrossRef]

78. Zhu, C.; Fang, C.; Zhang, L.; Wang, X. Simulating the interrelationships among population, water, ecology, and economy in urban agglomerations based on a system dynamics approach. *J. Clean. Prod.* **2024**, *439*, 140813. [CrossRef]

79. Wang, X.; Ding, Z. Analysis of network patterns and its influencing factors in Chengdu-Chongqing urban agglomeration based on multi-flow. *Heliyon* **2024**, *10*, e30375. [CrossRef] [PubMed]

80. Chen, C.; Zhong, Q.; Cao, Y.; Xu, G.; Chen, B. The Primacy Evaluation and Pattern Evolution Mechanism of the Central City in Nanjing Metropolitan Area. *Sustainability* **2024**, *16*, 8105. [CrossRef]

81. Wan, J.; Zhang, L.; Yan, J.; Wang, X.; Wang, T. Spatial–temporal characteristics and influencing factors of coupled coordination between urbanization and eco-environment: A case study of 13 urban agglomerations in China. *Sustainability* **2020**, *12*, 8821. [CrossRef]

82. Yuan, C.; Ma, N.; Xiong, X. The impact of urban growth boundary on urban sprawl: Evidence from China. *Reg. Environ. Chang.* **2024**, *24*, 157. [CrossRef]

83. Yang, Z.; Hua, Y.; Cao, Y.; Zhao, X.; Chen, M. Network patterns of zhongyuan urban agglomeration in China based on baidu migration data. *ISPRS Int. J. Geo-Inf.* **2022**, *11*, 62. [CrossRef]

84. Zhang, Y.; Wang, X.; Ji, M.; Chen, Y.; Yan, F. Evaluating the barrier of typical production factor flow in the Chengdu-Chongqing Urban Agglomeration based on multi-source big data. *Front. Environ. Sci.* **2022**, *10*, 1048378. [CrossRef]